World Journal of Advanced Engineering Technology and Sciences
eISSN: 2582-8266
Cross Ref DOI: 10.30574/wjaets
Journal homepage: https://wjaets.com/

(RESEARCH ARTICLE)

Computations of fields induced in biological tissues by electromagnetic (EM) wave in multilayered structure

Gasmelseed Akram *

College of Applied Medical Sciences, Qassim University, Saudi Arabia.

World Journal of Advanced Engineering Technology and Sciences, 2024, 13(01), 167–175

Publication history: Received on 27 July 2024; revised on 06 September 2024; accepted on 09 September 2024

Article DOI: https://doi.org/10.30574/wjaets.2024.13.1.0392

Abstract

The assessment of the fields induced in biological tissue by an electromagnetic (EM) wave is a major issue, not only for its relevance in medical research, but also for its implications on the setting of industrial standards. This paper describes the analysis of electromagnetic (EM) absorption properties of biological multilayered structure. The biological structure comprises three different tissues of skin, fat and muscle. A step-by-step approach for the computation of the EM fields within the multilayered structure is presented. The estimated specific absorption rate (SAR) distribution in tissues due to exposure from plane waves of frequencies 433, 900, 1300, 1800, and 2450 MHz, based on an incident power density 4.5 [mW/cm2], are also presented.

Keywords: Matrix formulation; Multilayered method; Recursive formulation; Specific absorption rate (SAR)

1. Introduction

There is close relationship between the mathematical description used in the biological model and the computational method for solving the EM fields inside the model. Thus, Computer modeling will likely remain the only viable method to determine the absorbed electromagnetic (EM) energy inside biological organs and tissues in many practical situations [1, 2].

Although, the availability of more powerful computers will allow for more realistic models [3–6], the biological model is not a unique object. It may have a different variety of forms and sizes. In these conditions no biological model should be considered as a representative model of the real biological target. Although medical imaging (e.g. CT or MRI) based anatomical models are realistically representing the bio-electromagnetic structure of the biological model, they require large computational resources for EM simulation. Thus, an attempt to directly analyze their electromagnetic absorption properties would be very difficult to carry out. It is therefore seems that simple models can be used satisfactorily to solve the absorption problem.

Although, modern numerical simulations are used effectively to determine internal field distribution for complex heterogeneous biological models, simple but important properties of the absorption can be illustrated by simple model [7 – 11]. Moreover, results from this simplified model can provide useful guidelines to workers frequently confronted with more complex EM absorption problems.

In this paper, the analysis of electromagnetic (EM) absorption properties of biological multilayered structure is described. The biological structure comprises three different tissues of skin, fat and muscle. A step-by-step approach for the computation of the EM fields within the multilayered structure is presented. The estimated specific absorption

* Corresponding author: Akram Gasmelseed

rate (SAR) distribution in tissues due to exposure from plane waves of frequencies 433, 900, 1300, 1800, and 2450 MHz, based on an incident power density 4.5 [mW/cm^2], are also presented.

2. Theory and calculations

Figure 1 shows the geometry of the problem. A plane wave is incident upon biological multilayered structure and traveling in the $+z$ -direction with the electric field $\overline{E}$ vector linearly polarized along the x -axis.

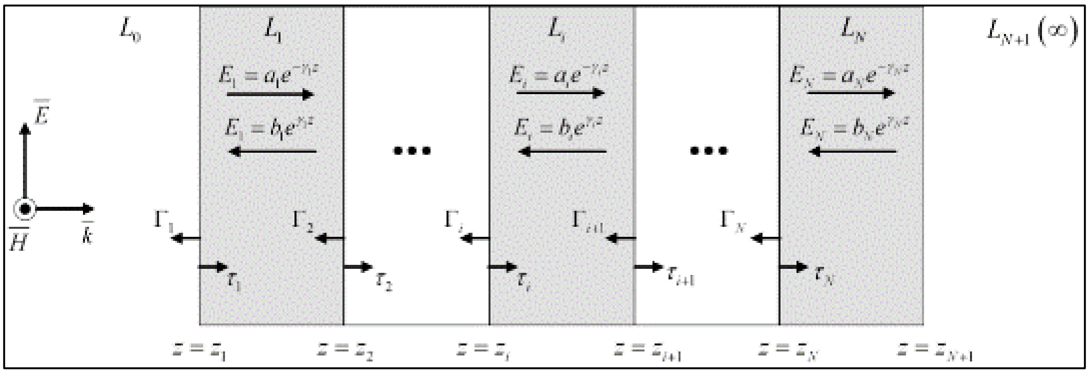

Figure 1 General biological multilayered structure

The incident field is assumed to have harmonic time variation $e^{j\omega t}$. There are $N+2$ layers $\left(L_0, L_1, \ldots, L_{N+1}\right)$, and $N+1$ interfaces $\left(z_1, z_2, \ldots, z_{N+1}\right)$. The ith layer indicated by L_i has permittivity ε_i [F/m], permeability μ_i [H/m], and conductivity σ_i [S/m]. Further, we denote the left-most layer (i.e. air) as L_0, while we denote the right-most layer by L_{N+1}. Then, the electric $\left(\overline{E}_i\right)$ and magnetic $\left(\overline{H}_i\right)$ fields in the ith layer are given by

$$\overline{E}_i = \left(a_i e^{-\gamma_i z} + b_i e^{\gamma_i z}\right) x \quad \ldots\ldots(1)$$

$$\overline{H}_i = \frac{\left(a_i e^{-\gamma_i z} - b_i e^{\gamma_i z}\right)}{\eta_i} y \quad \ldots\ldots(2)$$

where $i = 0, 1, \ldots, N+1$. The constant a_i and b_i are the amplitudes of incident and reflected waves, respectively. The amplitude of the incident electric field is represented by a_0, and is known in advance. γ_i and η_i denotes the propagation constant and the characteristic impedance L_i, respectively, and are given by

$$\gamma_i = \sqrt{j\omega\mu_i\left(\sigma_i + j\omega\varepsilon_i\right)} \quad \ldots\ldots(3)$$

$$\eta_i = \sqrt{\frac{\mu_i}{\varepsilon_i - j\left(\sigma_i / \omega\right)}} \quad \ldots\ldots(4)$$

Further, since the thickness of L_{N+1} is unlimited, $b_{N+1} = 0$. The input impedance of L_i denoted by r_i and is located at $z = z_i$, is given by

$$r_i = \frac{E_i(z)}{H_i(z)} = \eta_i \frac{\left(a_i e^{-\gamma z} + b_i e^{\gamma z}\right)}{\left(a_i e^{-\gamma z} - b_i e^{\gamma z}\right)} \quad \text{.....................} (5)$$

At the interface $z = z_i$, the reflection $\left(\Gamma_i\right)$ and transmission $\left(\tau_i\right)$ coefficients are given by

$$\Gamma_i = b_{i-1} / a_{i-1} \quad \text{....................}(6)$$

$$\tau_i = a_i / a_{i-1} \quad \text{........................} (7)$$

Dividing (5) by $a_i e^{-\gamma_i z_i}$ and substituting equation (6), we rewrite equation (5) as

$$r_i = \eta_i \frac{\left(1 + \Gamma_i e^{2\gamma_i z_i}\right)}{\left(1 - \Gamma_{i+1} e^{2\gamma_i z_i}\right)} \quad \text{.................} (8)$$

The unknown incident/reflected constants can be determined after imposing the continuity of the tangential components of the fields on the plane interfaces between the layers. Thus, due to the continuity of E_i and H_i across the interface $z = z_i$, the incident/reflected constants at the left of interface z_i are related to those at the left of interface z_{i+1} by

$$a_{i-1} e^{-\gamma_{i-1} z_i} + b_{i-1} e^{\gamma_{i-1} z_i} = a_i e^{-\gamma_i z_i} + b_i e^{\gamma_i z_i} \quad \text{.....................} (9)$$

$$\frac{a_{i-1} e^{-\gamma_{i-1} z_i} - b_{i-1} e^{\gamma_{i-1} z_i}}{\eta_{i-1}} = \frac{a_i e^{-\gamma_i z_i} - b_i e^{\gamma_i z_i}}{\eta_i} \quad \text{..............} (10)$$

By observing the relationship defined in equation (5), we may rewrite equation (10) as

$$\frac{a_{i-1} e^{-\gamma_{i-1} z_i} - b_{i-1} e^{\gamma_{i-1} z_i}}{\eta_{i-1}} = \frac{a_i e^{-\gamma_i z_i} + b_i e^{\gamma_i z_i}}{r_i} \quad \text{..................}(11)$$

Substituting equation (9) into equation (11) and dividing by a_{i-1} gives

$$\frac{e^{-\gamma_{i-1} z_i} - \Gamma_{i-1} e^{\gamma_{i-1} z_i}}{\eta_{i-1}} = \frac{e^{-\gamma_i z_i} + \Gamma_i e^{\gamma_i z_i}}{r_i} \quad \text{.........................}(12)$$

Solving equation (12) for Γ_i yields

$$\Gamma_i = \left[\frac{r_i - \eta_{i-1}}{r_i + \eta_{i-1}}\right] e^{-2\gamma_{i-1} z_i} \quad \text{.....................} (13)$$

Applying the relationship expressed in equation (6), we rewrite equation (9) as

$$a_{i-1}\left(e^{-\gamma_{i-1} z_i} + \Gamma_i e^{\gamma_{i-1} z_i}\right) = a_i \left(e^{-\gamma_i z_i} + \Gamma_{i+1} e^{\gamma_i z_i}\right) \quad \text{................} (14)$$

Thus, τ_i is given by

$$\tau_i = \frac{a_i}{a_{i-1}} = \frac{e^{-\gamma_{i-1}z_i} + \Gamma_i e^{\gamma_{i-1}z_i}}{e^{-\gamma_i z_i} + \Gamma_{i+1} e^{\gamma_i z_i}} \quad \text{……………. (15)}$$

Substituting equation (13) into (15) yields

$$\tau_i = \frac{2r_i}{r_i + \eta_{i-1}} \cdot \frac{e^{(\gamma_i - \gamma_{i-1})z_i}}{1 + \Gamma_{i+1} e^{2\gamma_i z_i}} \quad \text{……………….. (16)}$$

Conventionally, two approaches are used to calculate the electric and magnetic fields in the i[th] layer, L_i. In the first approach, the problem is solved recursively starting from the $N+1$ layer and ending to the 1[st] layer, whereas the second approach utilizes matrix theory.

2.1. Recursive formulation

In the last layer $N+1$, where waves exit the layered structure, there is only a forward traveling wave, or $b_{N+1} = 0$. Hence, it follows that $\Gamma_{N+2} = 0$. Thus, from (5), Z_{N+1} is equal to η_0, the characteristic impedance of free space. By using equations (4), (13), and (16) we compute Γ_{N+1} and τ_{N+1}. We repeat the procedure by computing Z_n, Γ_n, τ_n, and so on recursively, until Γ and τ have been evaluated at each interface. Then, we compute the complex constants, using equations (6) and (7). Finally, we use equations (1) and (2) to calculate the electric and magnetic fields in L_i [12 – 16].

2.2. Matrix formulation

The matrix formulation is particularly suited to compute the transmission of electromagnetic waves in multilayered structure. To better understand this formalism, let us consider a three multilayered structure which is similar to the one used in this paper, as shown in Figure 2.

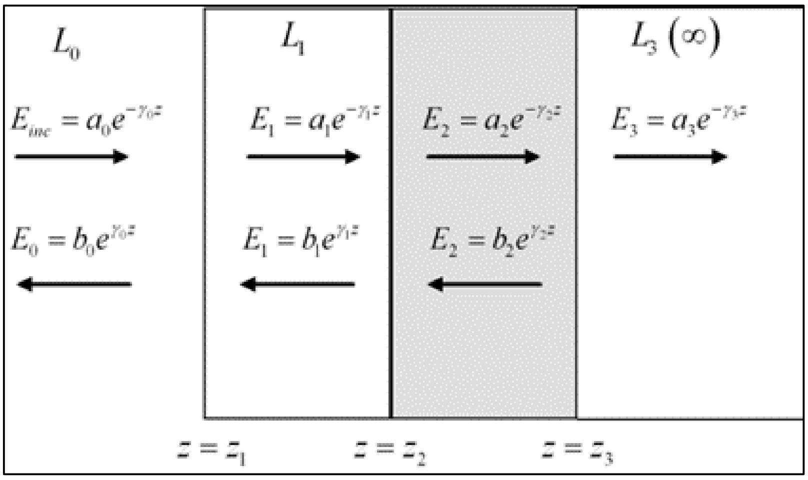

Figure 2 Three multilayered structure

The relation between the electric and magnetic fields at the interfaces can be expressed in matrix form as:

$$\begin{bmatrix} -1 & 1 & 1 & 0 & 0 & 0 \\ 1/\eta_1 & 1/\eta_2 & -1/\eta_2 & 0 & 0 & 0 \\ 0 & e^{-\gamma_2 z_2} & e^{\gamma_2 z_2} & -e^{-\gamma_3 z_2} & -e^{-\gamma_3 z_2} & 0 \\ 0 & e^{-\gamma_2 z_2}/\eta_2 & -e^{\gamma_2 z_2}/\eta_2 & -e^{-\gamma_3 z_2}/\eta_3 & e^{-\gamma_3 z_2}/\eta_3 & 0 \\ 0 & 0 & 0 & e^{-\gamma_3 z_3} & e^{\gamma_3 z_3} & -e^{-\gamma_4 z_3} \\ 0 & 0 & 0 & e^{-\gamma_3 z_3}/\eta_3 & -e^{\gamma_3 z_3}/\eta_3 & -e^{-\gamma_4 z_3}/\eta_4 \end{bmatrix} \cdot \begin{bmatrix} b_0 \\ a_1 \\ b_1 \\ a_2 \\ b_2 \\ a_3 \end{bmatrix} = \begin{bmatrix} a_0 \\ a_0/\eta_1 \\ 0 \\ 0 \\ 0 \\ 0 \end{bmatrix}$$

Finally, the electric and magnetic fields in L_i are obtained by taking the inverse of the matrix. Once the induced electric field inside the layered structure is known, the power density (W/m^3) absorbed along the ith layer from the sinusoidal field of amplitude E_i is given by

$$P_i = \frac{\sigma_i \left|E_i\right|^2}{2} \quad \text{.......................... (17)}$$

where σ_i is the conductivity of the ith layer (S/m), and E_i is the induced electric field (V/m). The rate of energy deposition by EM waves in tissue is characterized by specific absorption rate (SAR), which is specified in units Watt per Kilogram of tissue and given in terms of the electric field intensity as

$$SAR_i = \frac{P_i}{\rho_i} = \frac{\sigma_i}{\rho_i}\left|E_i\right|^2 \quad \text{................. (18)}$$

where ρ_i is the tissue density of the ith tissue layer (Kg/m^3).

3. Three layered tissue model

Figure 3, depicts a three layered dielectric structure, consisting of skin, fat, and muscle tissues, surrounded by free-space in which the permittivity and thickness of each layer is labeled. The electric field intensity E_i and SAR have been calculated in each layer for an incident power density of 4.5 [mW/cm^2] at 433, 900, 1300, 1800, and 2450 MHz. The incident power density P_{inc} is calculated using one of the following measurements units:

$$P_{inc} = a_0^2/377 \quad \left[W/m^2\right] \quad \text{.............. (19)}$$

$$P_{inc} = a_0^2/3770 \quad \left[mW/cm^2\right] \quad \text{.............. (20)}$$

where a_0 is the amplitude of the incident electric field intensity.

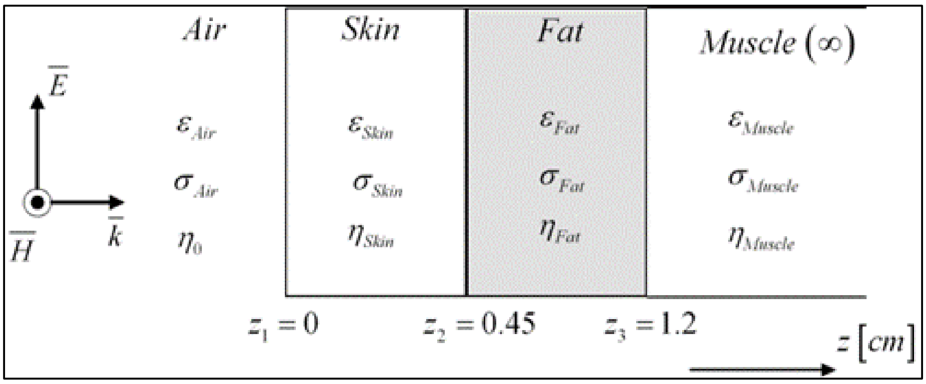

Figure 3 Skin-fat-muscle tissues model

Further, the dielectric properties of tissues are evaluated by use of the four-term Cole-Cole equation. A compilation of the EM properties of biological tissues at different frequencies is found in [17, 18]. The permittivity, conductivity and density of tissues are given in Table 1 for excitation frequencies equal to 433, 900, 1300, 1800, and 2450 MHz.

Table 1 Dielectric properties of skin-fat-muscle tissues model

Tissue	433 MHz		900 MHz		1.3 GHz		1.8 GHz		2.45 GHz		[3]ρ (Kg/m³)
	[1]ε_r	[2]σ	ε_r	σ	ε_r	σ	ε_r	σ	ε_r	σ	
Skin	46.08	0.702	41.41	0.867	39.92	1.001	38.87	1.185	38.01	1.464	1047
Fat	11.59	0.082	11.33	0.109	11.19	0.141	11.02	0.190	10.82	0.268	916
Muscle	57.73	0.826	55.96	0.969	55.19	1.132	54.44	1.389	53.57	1.81	1125

[1]ε_r: relative permittivity; [2]σ: conductivity [S/m]; [3]tissue density

The values of specific absorption rate (SAR) (Figures 5 and 6) have been calculated based on the calculation of the electric field strength distribution inside each layer of the structure shown in Figure 4. Figure 7 show the magnitude of reflection-coefficients.

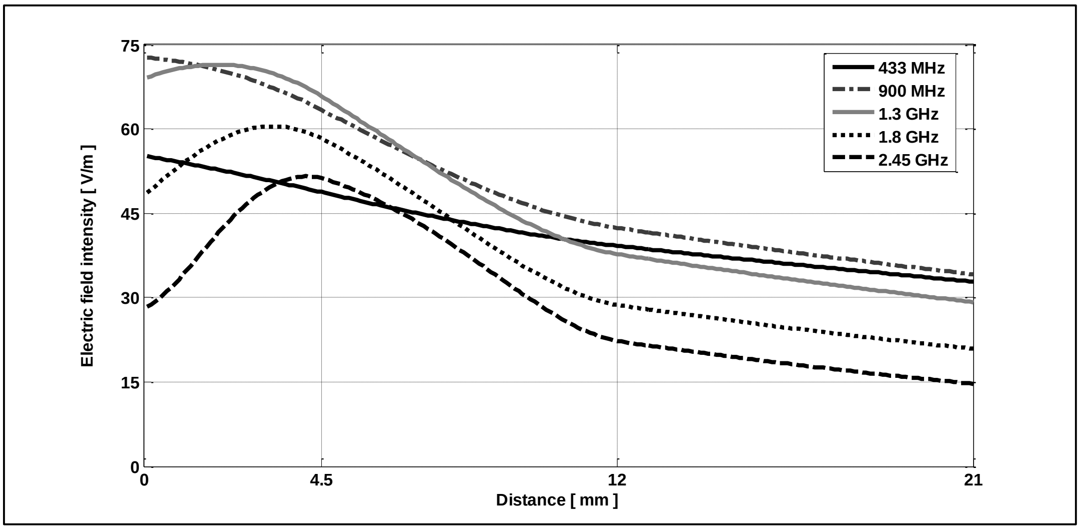

Figure 4 Electric field distributions in the layered structure

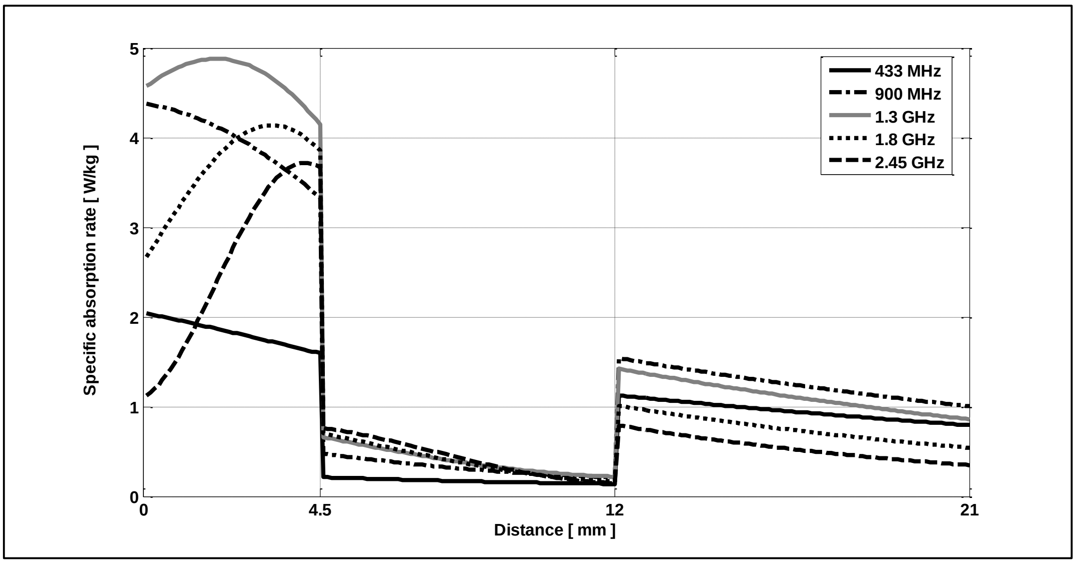

Figure 5 SAR distributions in the layered structure

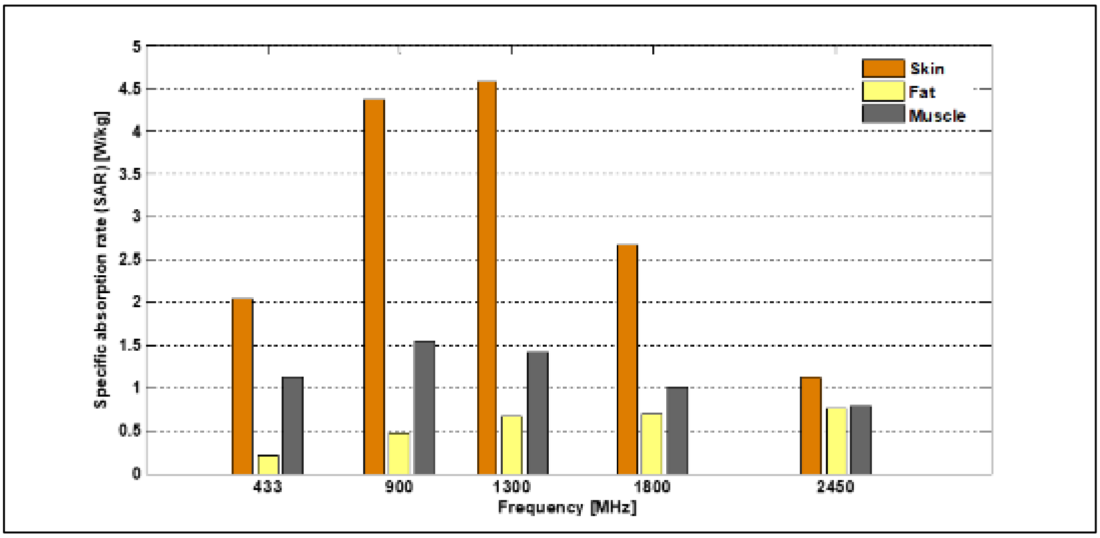

Figure 6 Magnitude of SAR [W/kg] for the different tissues in the model

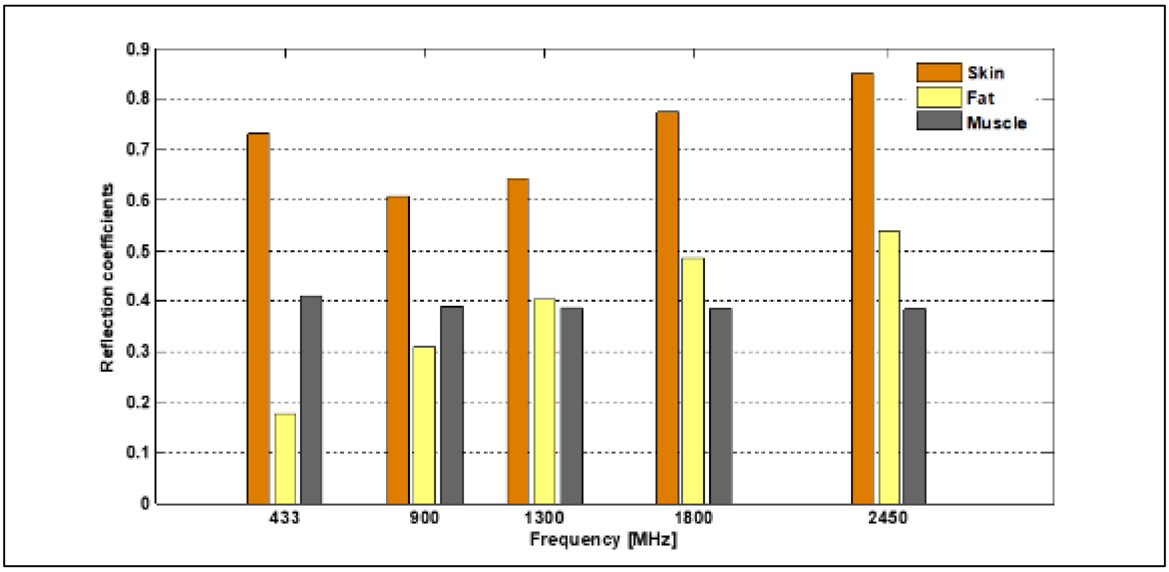

Figure 7 Magnitude of reflection coefficients Γ_i for the different tissues in the model

It is noted that the magnitude of SAR is minimum in the fat tissue (i.e. due to its poor conductivity) and maximum in the muscle tissue (i.e. due to its high conductivity) as shown in Figures 5 and 6. Further, Figure 6 indicates that the highest SAR values are observed at the skin layers of the layered structure at all frequencies. Moreover, of the three biological tissues examined, the highest SAR levels are seen to be at the skin layer of the structure at a frequency of 1.3 GHz.

These figures evidence the higher penetration depth at 900 MHz compared to 1800 MHz. In particular, at the frequency of 900 MHz about 26% of the incident power is transmitted. At frequency of 1800 MHz, about 10% of the incident wave is transmitted. In conclusion, at 1800 MHz the SAR increases with respect to the 900 MHz irradiation, while the SAR absorbed in the muscle reduces.

Further, our calculations show that the smallest SAR is in the fat tissue and it is approximately 0.2 W/kg and occurs at the lowest frequency of 433 MHz, which is a commonly used frequency for Industrial Scientific Medical (ISM) applicators [19]. Moreover, the SAR values are higher in the muscle tissue at 433 MHz compared with those at 2450 MHz. Generally, the higher the water content of a given tissue, the higher the dissipation of electromagnetic energy. Hence, fat tissue, which has low water content, is heated poorly compared to muscle tissue, which has higher water content. This is an important consideration in hyperthermia treatment [20 – 22], since the fat tissue will behave like a shielding structure and cause microwave power not be able to effectively penetrate into the muscle tissue to heat the tumor. Thus, the energy distribution may accumulate in the fat layer and cause heating damage to the fat tissue.

4. Conclusion

In this paper, the analysis of electromagnetic (EM) absorption properties of biological multilayered structure is described. The biological structure comprises three different tissues of skin, fat and muscle. The analysis and results presented here may be useful in designing applicators for hyperthermia treatment

References

[1] Derat B, Bolomy J. Various optimization problems of electromagnetic power absorption in homogeneous and heterogeneous phantoms. *IEEE Electromagnet. Compatibility* 2006; **48**: 641 – 647.

[2] Akram G, Jasmy Y. Numerical simulation of the FDTD method in LabVIEW. *IEEE Microwave Magazine* 2008. **8**: 90 – 99.

[3] Wang J, Fujiwara O. Dosimetry analysis and safety evaluation of realistic head models for portable telephones. *Transa. IEICE* 2000. **83**: 720 – 725.

[4] Nagaoka T, Watanabe S, Sakurai K, Kunieda E, Taki M, Yamanaka Y, Kitasalo C. Development of a realistic high resolution whole body voxel models of Japanese adult males and females of average height and weight, and application of models to radiofrequency EM field dosimetry. *Phys. Med. Biol.* 2004. **49**: 1 – 15.

[5] Onishi T, Ebara H, Pongpaibool P, Hamada L, Kiminami K, Uebayashi S, Watanabe S. RF dosimetry using Japanese anatomical models. *1st European Conf. on Antennas & Propagat. EuCAP* 2006. 1 – 4.

[6] Pisa S, Cavagnaro M, Lopresto V, Piuzzi E, Lovisolo G, Bernardi P. A procedure to develop realistic numerical models of cellular phones for an accurate evaluation of SAR distribution in the human head. *IEEE Trans. Microwave Theo. Tech.* 2005. **53**: 1256 – 1265.

[7] Samaras T, Christ A, Klingenbock A, Kuster N. Worst case temperature rise in a one-dimensional tissue model exposed to radiofrequency radiation*. IEEE Trans. Biomedical Eng.* 2007. **54**: 492 – 496.

[8] Eker S, Yeldiren B. Multi-layered lossy finite length dielectric cylindrical model of man at oblique incidence. *23rd IEEE annual Intl. Conf. of Eng. Medicine & Biol.* 2001. **4**: 4001 – 4004.

[9] Massoudi H, Durney C, Barber P, Iskandar M. Electromagnetic absorption in multi-layered cylindrical models of man. *IEEE Trans. Microwave Theo. Tech.* 1979. **27**: 825 – 830.

[10] Hombach V, Meier K, Burkhardt M, Kühn E, Kuster N. The dependence of EM energy absorption upon human head modeling at 900 MHz. IEEE *Trans. Microwave Theo. Tech.* 1996. **44**: 1865 – 1873.

[11] Baghdasaryan H, Knyazyan T. Problem of plane EM wave self-action in multilayer structure: an exact solution. *Optical & Quantum Electronics* 1999. **31**: 1059 – 1072.

[12] Akram G, Andrew T. A multilayered model of human head irradiated by electromagnetic plane wave of 100 MHz – 300 GHz. *Intl. Journal of Sci. Res.* 2006. **16**: 397 – 403.

[13] Drossos A, Santoma V, Kuster N. The dependence of Electromagnetic energy absorption upon human head tissue composition in the frequency range of 300 – 3000 MHz. *IEEE Trans. Microwave Theo. Tech.* 2000. **48**: 1988 – 1995.

[14] Pozar, D. *Microwave Engineering*. 2nd Ed. John Wiley & Sons, Inc. 1998.

[15] Akram G, Jasmy Y. LabVIEW-based multilayered model for estimation of the absorbed energy inside biological tissues. *IEEE Anten. & Propagat. Magazine 2008*. **50**: 152 – 158.

[16] Akram G, Jasmy Y. The effect of aging-related variations of normal human head on the induced specific absorption rate (SAR): plane multilayered head model. *IEEE Asia-Pacific Conf. on Appl. Electromag. APACE2007* 2007. 1 – 5.

[17] Gabriel C. , Gabriel S. Corthout E. The dielectric properties of biological tissues: I. Literature survey. *Phys. Med. Biol.* 1996. **41**: 2231 – 2249.

[18] Gabriel S, Lau R, Gabriel C. The dielectric properties of biological tissues: II. Measurements in the frequency range 10 Hz to 20 GHz. *Phys. Med. Biol.* 1996. **41**: 2251 – 2269.

[19] Bronzion J. *The biomedical engineering handbook*. 2nd ed. Boca Raton: CRC Press LLC, 2000.

[20] Sullivan D. Mathematical methods for treatment planning in deep regional hyperthermia. *IEEE Trans. Microwave Theo. Tech.* 1991. **39**: 864 – 872.

[21] Chuang H. Numerical computation of fat layer effects on microwave near-field radiation to the abdomen of a full-scale human body model. *IEEE Trans. Microwave Theo. Tech.* 1997. **45**: 118 – 125.

[22] Guy A. History of biological effects and medical applications of microwave energy. *IEEE Trans. Microwave Theo. Tech.* 1984. **32**: 1182 – 1200.